

NLO jet vertex from Lipatov's QCD effective action*

Martin Hentschinski & Agustín Sabio Vera

Instituto de Física Teórica UAM/CSIC, Nicolás Cabrera 15,
& Universidad Autónoma de Madrid, E-28049 Madrid, Spain

May 16, 2019

Real and virtual contributions to the quark-initiated forward jet vertex in QCD are calculated at next-to-leading logarithmic accuracy using Lipatov's effective action, valid in the high energy multi-Regge limit. A regularization of longitudinal divergencies is proposed which allows for the determination of jet observables. Agreement with previous results in the literature is found.

1 Introduction

Simplifications in scattering amplitudes of Quantum Chromodynamics (QCD) appear when the interaction takes place in the high energy Regge limit of large center-of-mass energy. For inelastic processes a generalization is to consider multi-Regge kinematics where the Regge limit is applied to multiple sub-channels [1]. Virtual contributions are then packed in a gluon Regge trajectory which appears as a $s_i^{\omega(t_i)}$ factor in each sub-channel with center-of-mass energy $\sqrt{s_i}$ and momentum transfer t_i . Reggeized gluons then naturally emerge in the t -channel with propagators indicating the no-emission probability of any particle in the rapidity interval $\sim \log(s_i/|t_i|)$. At the edge of these intervals emissions occur with a probability given by effective vertices representing the interaction of reggeons with usual particles. The gluon Regge trajectory $\omega(t_i)$ has been calculated at leading $\mathcal{O}(\alpha_s)$ (LL) and next-to-leading order $\mathcal{O}(\alpha_s^2)$ (NLL) in QCD and to all orders in $\mathcal{N} = 4$ super Yang-Mills theory [2]. At NLL, where terms of the form $(\alpha_s \log(s_i/t_i))^n$ and $\alpha_s (\alpha_s \log(s_i/t_i))^n$ are resummed, in each production cluster one or two particles can be generated, this is the so-called quasi-multi-Regge kinematics (QMRK) [3]. The linearity of QMRK is broken at higher orders due to unitarity in all channels, opening up transitions to multiple reggeized gluons in the t -channel.

The effective vertices for the coupling of reggeons to usual particles are complicated. An efficient tool to evaluate them is the high energy effective action proposed by Lipatov [4]. It is based on the QCD action with gauge fixing and ghost terms, with the addition of an induced component written in terms of gauge-invariant currents where Wilson lines generate color fields ordered in light cone components, with a non-trivial interaction with reggeon fields. Some transition vertices have been calculated using the Feynman rules derived from this effective action [4] (see also [5]). In the present work the focus lies on obtaining a vertex which is very important for phenomenological applications of QMRK to hadron colliders [6]: the vertex for the transition of a quark into a forward jet plus a remnant together with an off-shell reggeon in the t -channel. At the large hadron collider (LHC) at CERN there are several observables where QMRK should dominate. An example is that

*Preprint numbers: LPN11-55, IFT-UAM/CSIC-11-73, FTUAM-11-57

where jets are tagged in the forward region, with a relatively large transverse momentum. When two of these jets are each associated to one of the hadrons, and are at a large relative rapidity with similar transverse momentum squared, then QMRK applies. For the cross-section of this configuration the jet vertex studied in this work is a crucial piece. It is also possible to make the observable more exclusive by selecting events with a third jet in the central regions of rapidity at the detectors [7].

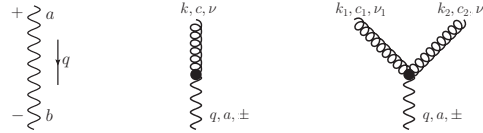
In this letter a first section is provided with a discussion on Lipatov's effective action together with the Feynman rules used in the subsequent calculations. The bulk of the results lie in the sections devoted to calculate the virtual and real corrections to the forward jet vertex, with a discussion on previous results in the literature. Finally, conclusions and suggestions for future work are presented.

2 High Energy Effective Action & Feynman Rules

The amplitudes of interest are the four-point amplitude with on-shell external quarks of momenta $p_a + p_b \rightarrow p_1 + p_2$, and the five-point amplitude with an extra on-shell gluon with momentum q in the final state. The squared center-of-mass energy is $s = (p_a + p_b)^2 = 2p_a \cdot p_b$. It is convenient to introduce the light-like four momenta n^\pm with $n^+ \cdot n^- = 2$ related to the incoming momenta by $n^+ = 2p_b/\sqrt{s}$ and $n^- = 2p_a/\sqrt{s}$. The Sudakov decomposition of a general vector k^μ , using $k^\pm \equiv k \cdot n^\pm$, is then $k^\mu = k^+ n^-/2 + k^- n^+/2 + k_\perp$, and $p_a = p_a^+ n^-/2, p_b = p_b^- n^+/2$.

With these notations at hand it is now possible to give a brief introduction to Lipatov's effective action, which contains two pieces. The first one is the usual QCD action with gauge fixing and ghost terms. The second one introduces new degrees of freedom, the gauge invariant reggeized gluon fields $A_\pm(x) = -it^a A_\pm^a(x)$, with t^a being the $SU(N_c)$ color matrices, and their interactions with the gluon fields $v_\mu(x) = -it^a v_\mu^a(x)$. The induced part of the effective action generates vertices with several reggeized gluons in the t -channel. To impose the condition that all gluon emissions with momenta q are ordered in longitudinal components ($q_i^+ \gg q_{i+1}^+, q_{i+1}^- \gg q_i^-$) the constraint $\partial_\pm A_\mp = 0$, with $\partial_\pm = n_\pm^\mu \partial_\mu$, is used. In QMRK clusters of particles are produced with a large rapidity distance between them. Inside each cluster the effective Lagrangian generating the interaction between reggeized and usual fields reads $\text{Tr} (V_+ \partial_\mu^2 A_- + V_- \partial_\mu^2 A_+)$ where $V_\pm = -g^{-1} \partial_\pm \text{P exp} \left(-\frac{g}{2} \int_{-\infty}^{x^\pm} dz^\pm v_\pm(z) \right)$ corresponds to an effective current formed by an array of fields ordered in longitudinal components.

The Feynman rules derived from this action can be found in [4]. The propagator for the reggeized gluon is simple. There also exists a direct transition vertex between a usual gluon and a reggeized one which can be understood as the projection of the standard gluon field on the kinematics and polarization of the reggeon field. Finally, for the calculations in this paper, the induced vertex for the gluon-gluon-reggeon transition is needed. These are graphically represented by



With the condition $q^\pm = 0$, the corresponding contributions are, respectively, $\frac{i}{2q_\perp^2} \delta_b^a$, $-iq_\perp^2 \delta_c^a (n^\pm)^\nu$ and $\frac{g}{2} f^{c_1 c_2 a} q_\perp^2 \left(\frac{1}{k_\perp^{\pm} + i\epsilon} + \frac{1}{k_\perp^{\pm} - i\epsilon} \right) (n^\pm)^{\nu_1} (n^\pm)^{\nu_2} (k_\perp^2 \text{ refers to Euclidean notation})$. In the last vertex a Cauchy principal value prescription has been introduced for the eikonal propagators which respects the original Bose symmetry of the induced vertices in the effective theory. These are all the pieces needed to perform the calculation of the quark-initiated jet vertex in this work.

The single tree level diagram for the four-point amplitude $p_a + p_b \rightarrow p_1 + p_2$ with the corresponding contribution of the coupling to the on-shell quarks reads

$$i\mathcal{M}_{qr^* \rightarrow q}^{(0)} = \bar{u}_{\lambda'}(p')igt^a \not{p}^\pm u(p)_\lambda = igt^a 2p^\pm \delta_{\lambda\lambda'}.$$

For dimension $d = 4 + 2\epsilon$, $C_F = \frac{N_c^2 - 1}{2N_c}$ and $\alpha_s = \frac{g^2 \mu^{2\epsilon} \Gamma(1-\epsilon)}{(4\pi)^{1+\epsilon}}$ the leading order quark impact factor $h_a^{(0)}(k_\perp)$ at cross section level $\left(d\hat{\sigma}_{qaqb}^{(0)} = h_a^{(0)}(k_\perp)h_b^{(0)}(k_\perp)d^{d-2}k_\perp\right)$ in $\overline{\text{MS}}$ scheme is then

$$|\overline{\mathcal{M}}^{(0)}|^2_{qr^* \rightarrow q} = \frac{1}{4N_c(N_c^2 - 1)} \sum_{\lambda\lambda'} |\mathcal{M}^{(0)}|^2_{qr^* \rightarrow q} = \frac{4g^2 C_F}{N_c^2 - 1} p_a^{+2}, \quad (1)$$

$$h_a^{(0)}(k_\perp) = \frac{\sqrt{N_c^2 - 1}}{(2p_a^+)^2} \int \frac{dk^-}{(2\pi)^{2+\epsilon}} \int \frac{d\Phi^{(1)}}{k_\perp^2} |\overline{\mathcal{M}}^{(0)}|^2_{qr^* \rightarrow q} = \frac{C_F}{\sqrt{N_c^2 - 1}} \frac{2^{1+\epsilon}}{\mu^{2\epsilon} \Gamma(1-\epsilon)} \frac{1}{k_\perp^2}, \quad (2)$$

which is in agreement with [8, 9].

3 Virtual Corrections

When calculating quantum corrections to the tree level result discussed above new divergencies in longitudinal components appear. In the present work these are regularized by going away from the light cone using a parameter ρ which is considered in the limit $\rho \rightarrow \infty$ and can be interpreted as a logarithm of the center-of-mass energy. In particular, the Sudakov projections take place on the vectors $n_a = e^{-\rho} n^+ + n_-$ and $n_b = n^+ + e^{-\rho} n^-$. To study the virtual corrections it is needed to obtain the one-loop self energy corrections to the reggeon propagator. Diagrammatically these are

In [...]₃ a ghost loop has been included. Keeping the leading ρ terms, using $\beta_0 = (11N_c - 2n_f)/3$ and $\lambda \equiv \frac{(-2ik_\perp^2)g^2 N_c}{(4\pi)^{2+\epsilon}} \left(\frac{k_\perp^2}{\mu^2}\right)^\epsilon \frac{\Gamma(1-\epsilon)\Gamma(1+\epsilon)^2}{\Gamma(1+2\epsilon)}$, each contribution and the full result are

$$\begin{aligned} \text{Diagram} &= \lambda \left\{ \left[\frac{2\rho - i\pi}{\epsilon} \right]_1 + \frac{1}{(1+2\epsilon)\epsilon} \left(\left[1 \right]_2 - \left[\frac{3\epsilon + 5}{3 + 2\epsilon} \right]_3 + \frac{n_f}{N_c} \left[\frac{2 + 2\epsilon}{3 + 2\epsilon} \right]_4 \right) \right\} \\ &= \frac{\alpha_s N_c (-2ik_\perp^2)}{2\pi} \left(\frac{k_\perp^2}{\mu^2} \right)^\epsilon \left(\frac{i\pi - 2\rho}{2\epsilon} - \frac{\beta_0}{2N_c\epsilon} + \frac{67}{18} + \frac{10n_f}{18N_c} \right) + \mathcal{O}(\epsilon). \end{aligned} \quad (3)$$

From the effective action the one-loop corrections to the $i\mathcal{M}_{qr^* \rightarrow q}^{(1)}$ quark-quark-reggeon vertex are

$$\begin{aligned}
&= \left[\text{Diagram 1} \right]_1 + \left[\text{Diagram 2} \right]_2 + \left[\text{Diagram 3} \right]_3 \\
&+ \left[\text{Diagram 4} \right]_4 + \left[\text{Diagram 5} \right]_5 + \left[\text{Diagram 6} \right]_6 \\
&= \frac{i\mathcal{M}_{qr^* \rightarrow q}^{(0)}}{(-2ik_{\perp}^2)} \frac{\lambda}{\epsilon} \left\{ \left[\frac{1}{\epsilon} - 2 \ln \frac{p_a^+}{\sqrt{k_{\perp}^2}} - 2\rho + i\pi - \psi(1-\epsilon) - \psi(1) + 2\psi(\epsilon) \right]_1 \right. \\
&\quad \left. + \frac{1}{(1+2\epsilon)} \left(\left[\frac{1}{2} \right]_2 + \frac{1}{N_c^2} \left[\frac{2+\epsilon+2\epsilon^2}{2\epsilon} \right]_3 - \left[\frac{3\epsilon+5}{3+2\epsilon} \right]_4 - \left[1 \right]_5 + 2 \frac{n_f}{N_c} \left[\frac{1+\epsilon}{3+2\epsilon} \right]_6 \right) \right\} \\
&= \frac{i\mathcal{M}_{qr^* \rightarrow q}^{(0)}}{(-2ik_{\perp}^2)} \frac{\lambda}{\epsilon} \left\{ - \left(\ln \frac{-p_a^+}{\sqrt{k_{\perp}^2}} + \ln \frac{p_a^+}{\sqrt{k_{\perp}^2}} + \rho \right) - \frac{1}{(1+2\epsilon)} \left[- \frac{1}{N_c^2} \left(\frac{1}{\epsilon} + \frac{1+2\epsilon}{2} \right) \right. \right. \\
&\quad \left. \left. + \frac{11+7\epsilon}{3+2\epsilon} - 2 \frac{n_f}{N_c} \frac{1+\epsilon}{3+2\epsilon} - \frac{2+7\epsilon}{2\epsilon} + (1+2\epsilon) \left(\psi(1-\epsilon) - 2\psi(\epsilon) + \psi(1) \right) \right] \right\}, \quad (4)
\end{aligned}$$

where $\psi(z) = \Gamma'(z)/\Gamma(z)$. From this result it is now needed to subtract the non-local contributions stemming from the one-loop corrections to the reggeon propagator:

$$\begin{aligned}
&= i\mathcal{M}_{qr^* \rightarrow q}^{(0)} \frac{g^2}{(4\pi)^{2+\epsilon}} \left(\frac{k_{\perp}^2}{\mu^2} \right)^{\epsilon} \frac{\Gamma(1-\epsilon)\Gamma^2(1+\epsilon)}{\Gamma(1+2\epsilon)} \left\{ \frac{-2N_c}{\epsilon} \left(\ln \frac{p_a^+}{\sqrt{k_{\perp}^2}} - \frac{\rho}{2} \right) \right. \\
&\quad \left. + \frac{N_c(2+7\epsilon)}{2\epsilon^2(1+2\epsilon)} \frac{1}{N_c} \left(\frac{1}{\epsilon^2(1+2\epsilon)} + \frac{1}{2\epsilon} \right) - N_c \frac{1}{\epsilon} \left(\psi(1-\epsilon) - 2\psi(\epsilon) + \psi(1) \right) \right\}. \quad (5)
\end{aligned}$$

The four-point elastic amplitude is the sum of two contributions as the one calculated above:

$$i\mathcal{M}_{q_a q_b \rightarrow q_1 q_2}^{(1)} = \text{Diagram 1} + \text{Diagram 2} + \text{Diagram 3} + \text{Diagram 4},$$

where the ρ dependence cancels while the terms with $\ln p_a^+/\sqrt{k_{\perp}^2}$ and $\ln p_b^-/\sqrt{k_{\perp}^2}$ generate the LL contribution of the form $(\omega(-k_{\perp}^2) = -\frac{\alpha_s N_c}{2\pi} \left(\frac{1}{\epsilon} + \ln \frac{k_{\perp}^2}{\mu^2} \right))$ is the LL gluon Regge trajectory)

$$i\mathcal{M}_{q_a q_b \rightarrow q_1 q_2}^{(1)} = i\mathcal{M}_{q_a q_b \rightarrow q_1 q_2}^{(0)} \left(\frac{1}{2} \left(\ln \frac{s}{k_{\perp}^2} + \ln \frac{-s}{k_{\perp}^2} \right) \omega(-k_{\perp}^2) + \Gamma_a^{(1)}(k_{\perp}^2) + \Gamma_b^{(1)}(k_{\perp}^2) \right). \quad (6)$$

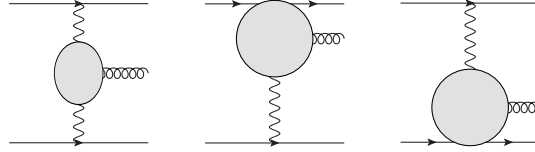
This piece is associated to the reggeon exchange and is removed from the quark-quark-reggeon vertex corresponding to the coupling to the external fields, which hence reads

$$\Gamma_{a,b}^{(1)}(k_\perp^2) = \frac{\alpha_s}{2} \left(\frac{k_\perp^2}{\mu^2} \right)^\epsilon \left[\frac{N_c}{\pi} \left(\frac{85}{36} + \frac{\pi^2}{4} \right) - \frac{\beta_0}{4\pi\epsilon} - \frac{C_F}{\pi} \left(\frac{1}{\epsilon^2} - \frac{3}{2\epsilon} + 4 - \frac{\pi^2}{6} \right) \right]. \quad (7)$$

This result is in perfect agreement with the more standard calculations, not using the high energy effective action, performed in [10] and confirmed in [11].

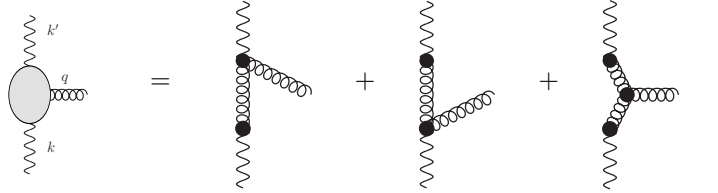
4 Real Corrections

The real corrections to the Born level process can be organized into three contributions to the five-point amplitude with central and quasi-elastic gluon production, *i.e.*,



To regularize the divergencies appearing in the integration over the longitudinal phase space of the gluon an explicit cut-off in rapidity will be used for the intermediate steps in the calculation.

The central production amplitude yields the unintegrated real part of the forward leading order BFKL kernel and is obtained from the sum of the following three effective diagrams:



The Sudakov decomposition of the external momenta is $k'_\perp = q^+ n^+ / 2 + q_\perp - k_\perp$, $k = k^- n^+ / 2 + k_\perp$ and $q = q^+ n^+ / 2 + k^- n^+ / 2 + q_\perp$, with $k^- = q_\perp^2 / q^+$. The squared amplitude, averaged over color of the incoming reggeons and summed over final state color and helicities reads

$$\overline{|\mathcal{M}|^2}_{r^* r^* \rightarrow g} = \frac{16g^2 N_c}{N_c^2 - 1} \frac{(q_\perp - k_\perp)^2 k_\perp^2}{q_\perp^2}. \quad (8)$$

It leads to the following production vertex

$$V(k_\perp, k'_\perp) = \frac{N_c^2 - 1}{8(2\pi)^{3+2\epsilon} k_\perp'^2 k_\perp^2} \overline{|\mathcal{M}|^2}_{r^* r^* \rightarrow g} = \frac{\alpha_s N_c}{\pi_\epsilon \pi (k_\perp + k'_\perp)^2}, \quad (9)$$

with $\pi_\epsilon \equiv \pi^{1+\epsilon} \Gamma(1-\epsilon) \mu^{2\epsilon}$ and momentum conservation and on-shellness implied. Finally, the central production contribution to the exclusive differential cross section is

$$d\hat{\sigma}_{ab}^{(c)} = h_a^{(0)}(k'_\perp) h_b^{(0)}(k_\perp) \mathcal{V}(q_\perp; k_\perp, k'_\perp) d^{2+2\epsilon} k'_\perp d^{2+2\epsilon} k_\perp d\eta, \quad (10)$$

with $\mathcal{V}(q_\perp; k_\perp, \eta_a, \eta_b) \equiv V(q_\perp; k_\perp, k'_\perp) \theta(\eta_a - \eta) \theta(\eta - \eta_b)$ being the regularized production vertex. The quasi-elastic contribution $q(p_a) r^*(k) \rightarrow g(q) q(p)$ is the sum of the effective diagrams



The Sudakov decomposition $p = (p_a^+ - q^+)n^-/2 + p^-n^+/2 + k_\perp - q_\perp$, $q = q^+n^-/2 + (k^- - p^-)n^+/2 + q_\perp$, with $p^- = (k_\perp - q_\perp)^2/((1-z)p_a^+)$, $k^- = (\Delta_\perp^2 + z(1-z)k_\perp^2)/((1-z)zp_a^+)$, $z = q^+/p_a^+$ and $\Delta_\perp \equiv q_\perp - zk_\perp$, is used to obtain the squared amplitude

$$|\overline{\mathcal{M}}|^2_{r^*q \rightarrow qg} = \frac{g^4 8p_a^+}{N_c^2 - 1} \frac{\mathcal{P}_{gq}(z, \epsilon)}{\Delta_\perp^2 q_\perp^2} \frac{(1-z)zk_\perp^2}{k_\perp'^2} \left[C_F z^2 k_\perp'^2 + N_c(1-z)\Delta_\perp \cdot q_\perp \right] \theta \left(z - e^{-\eta_b} \frac{\sqrt{q_\perp^2}}{p_a^+} \right), \quad (11)$$

where $\mathcal{P}_{gq}(z, \epsilon) = C_F \frac{1+(1-z)^2+\epsilon z^2}{z}$ is the real part of the $q \rightarrow g$ splitting function and η_b a lower cut-off in rapidity. To wrap up, the real corrections to the impact factor are then

$$h^{(1)}(k_\perp) dz d^{2+2\epsilon} q_\perp = \frac{\sqrt{N_c^2 - 1}}{(2p_a^+)^2} \int \frac{dk^-}{(2\pi)^{2+\epsilon}} d\Phi^{(2)} |\mathcal{M}|_{qg^* \rightarrow qg}^2 \frac{1}{k_\perp^2}, \quad (12)$$

with the two-particle phase space being

$$d\Phi^{(2)} = \frac{1}{2p_a^+ (2\pi)^{2+2\epsilon}} dz d^{2+2\epsilon} q_\perp \frac{1}{(1-z)z} \delta \left(k^- - \frac{\Delta_\perp^2 + z(1-z)k_\perp^2}{(1-z)p_a^+} \right). \quad (13)$$

The final result exactly agrees with the equivalent one in [9]:

$$h^{(1)}(k_\perp) = h^{(0)}(k_\perp) \frac{\alpha_s}{2\pi} \frac{\mathcal{P}_{gq}(z, \epsilon)}{\pi_\epsilon} \frac{1}{q_\perp^2 \Delta_\perp^2} \left[C_F z^2 k_\perp'^2 + N_c(1-z)\Delta_\perp \cdot q_\perp \right] \theta \left(z - e^{-\eta_b} \frac{\sqrt{q_\perp^2}}{p_a^+} \right). \quad (14)$$

To construct the complete differential cross section it is now needed to subtract the contribution from gluon production at central rapidities:



In this way the quasi-elastic contribution to the exclusive differential cross-section is

$$d\hat{\sigma}_{ab}^{(qea)} = h_a^{(0)}(k'_\perp) h_b^{(0)}(k_\perp) \mathcal{G}_{qqg}(k_\perp, q_\perp, z, \eta_a, \eta_b) d^{2+2\epsilon} q_\perp d^{2+2\epsilon} k_\perp dz \quad (15)$$

where

$$\begin{aligned} \mathcal{G}_{qqg} \equiv & \frac{\alpha_s}{2\pi} \left\{ \frac{\mathcal{P}_{gq}(z, \epsilon)}{\pi_\epsilon} \left[\frac{C_F z^2 k_\perp'^2}{q_\perp^2 \Delta_\perp^2} + \frac{N_c(1-z)\Delta_\perp \cdot q_\perp}{q_\perp^2 \Delta_\perp^2} - \frac{N_c}{z} \frac{1}{k_\perp'^2} \right] \right\} \theta \left(z - e^{-\eta_b} \frac{\sqrt{q_\perp^2}}{p_a^+} \right) \\ & + \frac{N_c}{z} \frac{1}{k_\perp'^2} \theta \left(z - e^{-\eta_b} \frac{\sqrt{q_\perp^2}}{p_a^+} \right) \theta \left(z - e^{\eta_a} \frac{\sqrt{q_\perp^2}}{p_a^+} \right). \end{aligned} \quad (16)$$

The complete exclusive differential cross-section is then given as the sum of central and quasi-elastic contributions:

$$d\hat{\sigma}_{ab} = d\hat{\sigma}_{ab}^{(c)} + d\hat{\sigma}_{ab}^{(qea)} + d\hat{\sigma}_{ab}^{(qeb)}. \quad (17)$$

5 Conclusions and Outlook

In this letter an advanced application of Lipatov's effective action for the description of QCD processes at high energies is explained in detail. The calculation of the most interesting jet vertex for applications to hadronic phenomenology has been performed, finding precise agreement with previous results in the literature, obtained with more conventional approaches. A particular regularization of longitudinal divergencies has been proposed which allows for the determination of NLL matrix elements. Applications of this technique to other processes and, in particular, to the extraction of the gluon-initiated jet vertex and two-loop gluon Regge trajectory are being carried out in a parallel work.

Acknowledgements Discussions with our collaborators J. Bartels and L. Lipatov are acknowledged. Research partially funded by European Commission (LHCPhenoNet PITN-GA-2010-2645649), Comunidad de Madrid (HEPHACOS ESP-1473) and German Academic Exchange Service (DAAD).

References

- [1] L. N. Lipatov, Sov. J. Nucl. Phys. **23** (1976) 338, E. A. Kuraev, L. N. Lipatov, V. S. Fadin, Phys. Lett. B **60** (1975) 50, Sov. Phys. JETP **44** (1976) 443, Sov. Phys. JETP **45** (1977) 199; I. I. Balitsky, L. N. Lipatov, Sov. J. Nucl. Phys. **28** (1978) 822.
- [2] V. S. Fadin, R. Fiore, M. I. Kotsky, Phys. Lett. **B387** (1996) 593-602. A. V. Kotikov, L. N. Lipatov, Nucl. Phys. **B582** (2000) 19-43. J. Bartels, L. N. Lipatov, A. Sabio Vera, Phys. Rev. **D80** (2009) 045002, Eur. Phys. J. **C65** (2010) 587-605.
- [3] Fadin, Lipatov, Phys. Lett. B **429** (1998) 127; Ciafaloni, Camici, Phys. Lett. B **430** (1998) 349.
- [4] L. N. Lipatov, Nucl. Phys. **B452** (1995) 369-400, Phys. Rept. **286** (1997) 131-198. E.N.Antonov, L.N.Lipatov, E.A.Kuraev, I.O.Cherednikov, Nucl. Phys. **B721** (2005) 111-135.
- [5] M. Hentschinski, Acta Phys. Polon. **B39** (2008) 2567-2570; arXiv:0908.2576 [hep-ph]; Nucl. Phys. Proc. Suppl. **198** (2010) 108-111. M. Hentschinski, J. Bartels, L. N. Lipatov, [arXiv:0809.4146 [hep-ph]].
- [6] A.Sabio Vera, Nucl.Phys.B **746**, 1 (06), A.Sabio Vera, F.Schwennsen, N.Phys.B **776**, 170 (07). D. Colferai, F. Schwennsen, L. Szymanowski, S. Wallon, JHEP **1012** (2010) 026. M. Angioni, G. Chachamis, J. D. Madrigal, A. Sabio Vera, [arXiv:1106.6172 [hep-th]].
- [7] J. Bartels, A. Sabio Vera, F. Schwennsen, JHEP **0611** (2006) 051. M. Deak, F. Hautmann, H. Jung, K. Kutak, arXiv:1012.6037 [hep-ph].
- [8] M.Ciafaloni, D.Colferai, Nucl.Phys.**B538** (99) 187. M.Ciafaloni, Phys.Lett.**B429** (98) 363.
- [9] J. Bartels, D. Colferai, G. P. Vacca, Eur. Phys. J. C **24** (2002) 83.
- [10] V. S. Fadin, R. Fiore, A. Quartarolo, Phys. Rev. D **50** (1994) 2265.
- [11] V. Del Duca, C. R. Schmidt, Phys. Rev. D **57** (1998) 4069.